AFOSR-TR-97

0537

REPORT DOCUMENTATION PAGE

1. AGENCY USE ONLY (Leave Blank)	2. REPORT DATE	3. REPORT TYPE AND DATES COVERED
	7/30/97	Final Report 9/1/95 - 7/30/97

4. TITLE AND SUBTITLE Application of Micro Electro-Mechanical Sensors and Activators in the Investigation of Supersonic Jet Screech.

5. FUNDING NUMBERS

AFOSR
F49620-93-1-0459

6. AUTHOR(S)

Hassan Nagib
Ahmed Naguib
Joe Papp

7. PERFORMING ORGANIZATION NAME(S) AND ADDRESS(ES)

Fluid Dynamics Research Center
Illinois Institute of Technology
10 W. 32nd Street
Chicago, IL 60616

8. PERFORMING ORGANIZATION REPORT NUMBER

9. SPONSORING / MONITORING AGENCY NAME(S) AND ADDRESS(ES)

AFOSR/NA
110 Duncan Ave. Suite B115
Bolling AFB, DC 20332-0001

10. SPONSORING / MONITORING AGENCY REPORT NUMBER

19971021 257

11. SUPPLEMENTARY NOTES

a. DISTRIBUTION / AVAILABILITY STATEMENT

Approved for public release.

12. DISTRIBUTION CODE

13. ABSTRACT *(Maximum 200 words)*

An investigation aimed at examining the usability of MEMS-based actuators for controlling supersonic jet screech has been conducted. First, documentation of the screech phenomenon in the newly constructed high-speed jet facility (HSJF) at IIT has been completed. Results from microphone measurements complemented with earlier shadowgraph and schlieren visualization have shown that the screech characteristics in the HSJF conforms with that published in the literature.

Second, detailed investigation of the first-generation MEMS actuators showed that the actuators could not operate for speeds higher than 70 m/s while maintaining "contact" with the jet shear layer. This was attributed to the bending moment acting on the actuator due to flow loading on the overhanging head-portion of the device. This observation was confirmed utilizing a special "headless" actuator design. The outcome of the tests of the first-generation devices guided the development of a second-generation of actuators. Those actuators, which are also described within this report, are currently being evaluated.

14. SUBJECT TERMS

MEMS
Supersonic Jet Screech

15. NUMBER OF PAGES

13

16. PRICE CODE

17. SECURITY CLASSIFICATION OF REPORT	18. SECURITY CLASSIFICATION OF THIS PAGE	19. SECURITY CLASSIFICATION OF ABSTRACT	20. LIMITATION OF ABSTRACT
Unclassified	Unclassified	Unclassified	UL

APPLICATION OF MICRO-ELECTRO-MECHANICAL SENSORS AND ACTUATORS IN THE INVESTIGATION OF SUPERSONIC JET SCREECH

FINAL REPORT

JUNE 1997

AFORSR-49620-93-1-0459

INVESTIGATORS:

Hassan M. Nagib

Ahmed M. Naguib

ILLINOIS INSTITUTE OF TECHNOLOGY

Fluid Dynamics Research Center

&

Mechanical and Aerospace Engineering Department

Chicago, Illinois 60616

OBJECTIVES

This work has several objectives:

1. Identify the screech phenomenon in a new anechoic high-speed jet facility (HSJF) at IIT.
2. Acquire information to aid in the design of MEMS devices for the purpose of generating shear layer disturbances.
3. Design a MEMS array that will ultimately be used for the purpose of interrupting the screech feedback loop at the point of receptivity.
4. Evaluate the effectiveness of the MEMS actuators in exciting the high-speed jet shear layer.

PROGRESS AND DISCUSSION

2.1. Identification of the screech phenomenon in the HSJF. In the last progress report on this grant, we reported on a non-intrusive high-speed schlieren and shadowgraph system which was used to visualize the jet shear layer and the shock cell system in the HSJF during screech for a range of fully expanded Mach numbers. Since then, we have conducted detailed microphone measurements to identify and compare the frequency and mode of screech in the HSJF to published information. Furthermore, we were able to make some comparisons between the flow visualization and microphone results as will be explained below.

To document the screech frequency in the HSJF, acoustic spectra were calculated from data acquired using 1/8 inch condenser microphone at a location 8.5 diameters from the jet axis in the radial direction and 1.5 diameters downstream of the nozzle lip. The open circles in Figure 1 show the resulting plot of fundamental frequency versus Mach number. The plot is divided into four main regions of smooth change using a convention similar to that used by Powell (1953) and Merle (1955). In this convention, the stages or modes of screech were labeled A_1, A_2, B, C and D. Here mode D was beyond the range of the pressure transducer used in the current study.

Figure 2 shows the current results as well as data from similar experiments made by Powell (1953) and Tam (1994). Good agreement is shown apart from the location of the transition between modes B and C. It is generally accepted that this transition point is particular to each facility and may be a measure of the turbulence level of the facility, as

suggested by Davis and Oldfield (1962). Also shown in Figure 2 is a line representing the screech frequency model proposed by Tam et al. (1986).

Close inspection of Figure 3, where a shadowgraph image of the jet flow at a fully expanded Mach number (M_j) of 1.12 is shown, reveals corrugated patterns perpendicular to the flow direction near the nozzle exit. These features appear to be characteristic of Kelvin-Helmholtz instabilities of the shear layer. If the wavelength of these features is measured from the shadowgraph image and their convection velocities are assumed to be half of the fully expanded jet velocity then a rough estimate of the frequency of the presumed Kelvin-Helmholtz instabilities can be made. In the case of Figure 3, the estimated frequency is approximately 8.4 kHz. The same procedure for identifying the passage frequency of the shear layer structures was repeated at two other Mach numbers. The results are compared to the acoustic frequency of screech in Figure 1 (where the closed circles represent the passage frequency of the shear layer structures). As seen from the figure, a good agreement between the screech and vortical-passage frequency is obtained. This provides evidence that the observed large-scale disturbances are those involved in the screech feedback loop.

2.2. Evaluation of the first generation of the MEMS actuators. In the last progress report, results for some limited testing of the first-generation MEMS actuators were reported. Then, it was shown that the actuators ceased to operate well outside the high-speed shear layer during the course of the experiments. This was thought to be due to the lateral forces on the actuator caused by fluid entrainment by the jet flow. However, the actuator was shown to be able to excite the jet shear layer at a low speed of about 20 m/s.

Sine the last report, we have made systematic testing of the first generation of actuators while varying the flow speed and the actuator location with respect to the nozzle lip. However, before reporting on those results, a brief description of the MEMS actuator will be made for the purpose of self containment. Figure 4 provides a SEM view of the first generation actuator design. The device consists of a free-floating section and a section which is bonded to the glass substrate. The free-floating and bonded sections are connected via a folded-beam structure. The actuator is made to oscillate by applying an AC voltage to the comb structure shown in Figure 4. The frequency of the forcing voltage is set to be equal to the resonant frequency of the actuator; i.e., 5 kHz.

To examine the ability of the actuator to operate at different jet velocities, the actuator was tested at speeds up to 100 m/s. It was observed that as the speed increases, the ability of the actuator to operate in the vicinity of the jet lip was reduced. In particular, Figure 5 shows the radial position of the actuator with respect to the jet lip at which the actuator stops moving as a function of the jet speed. Note that in Figure 5 positive values of the radial position correspond to the actuator being inside the shear layer, while negative values represent locations away from the flow. It is seen from the figure that at jet speeds of 70 m/s or higher the actuators cannot operate in direct "contact" with the shear layer. This suggests that the actuator is being stopped by the moment delivered to the overhanging portion of the device, as it penetrates the flow.

To test this theory further, several devices were manufactured which had their overhanging portions removed. These were termed "headless" actuators. A device of this kind was able to operate at closer distances to the nozzle lip than the devices with the head. This provided additional evidence of the effect of the flow-induced moment on the actuator operation.

Notwithstanding the ability of the actuators to operate up to a jet speed of 70 m/s while protruding into the flow, this first generation of actuators was able to excite the shear layer only up to a jet speed of 35 m/s. This is demonstrated from the sample spectrum measurements shown in Figures 6 and 7 at jet speeds of 35 and 43 m/s, respectively. As seen from Figures 6, only a small peak in the disturbance streamwise velocity spectrum is detected in the shear layer at the MEMS forcing frequency for 35 m/s jet speed. At a jet speed of 43 m/s (Figure 7) no MEMS-induced disturbance is observed in the velocity spectrum.

2.3. The second-generation MEMS actuators. Based on the test results of the first-generation actuators, it became clear that the actuator stiffness in the plane parallel to the jet flow direction needed to be increased. To this end, a second-generation of actuators was designed and fabricated. An SEM view of the new actuator is shown in Figure 8. In comparison with the first-generation actuators, the second actuator design incorporated three main modifications:

1. The support anchors for the movable part of the actuator were spread out over the entire area of the actuator, thus effectively increasing the torsional stiffness of the actuator.
2. The distance from the anchors to the two ends of the actuator was reduced from about 400 μm to about 200 μm.
3. The dynamic loading on the actuator head was reduced by creating holes in the overhanging actuator tip.

The new design is predicted to have about an order of magnitude better stiffness in the direction of the flow than the first design. The second-generation devices are currently being tested and evaluated in the HSJF.

REFERENCES

Davis, M. G. and Oldfield, D. E. S. 1962. "Tones from a Choked Axisymmetric Jet", *Acustica*, **Vo. 12**, No.4, pp. 257-277.

Merele, M. 1955. "Ondes Sonores Emises par un Jet d'Air", *Academic des Sciences, Comptes Rendus*, **Vol. 240**, pp. 2055-2057.

Powell, A. 1953. "On the Noise Emanating from a Two-Dimensional Jet above the Critical Pressure", *The Aeronautical Quarterly*, **Vol. 4**, pp. 103-120, 1953.

Tam, C. K. W., Seiner, J. M., and Yu, J. C. 1986. "Proposed Relationship Between Broadban Shock Associated Noise and Screech Tones", *Journal of Sound and Vibration*, **Vol. 110**, No. 2, pp. 309-321.

Tam, C. K. W. 1994. "Screech Tones from Free and Ducted Supersonic Jets", *AIAA Journal*, **Vo. 1**, No. 3, pp. 429-444, 1977.

PERSONNEL SUPPORTED

Graduate Students: Joe Papp

PUBLICATIONS

None

TRANSITIONS

None

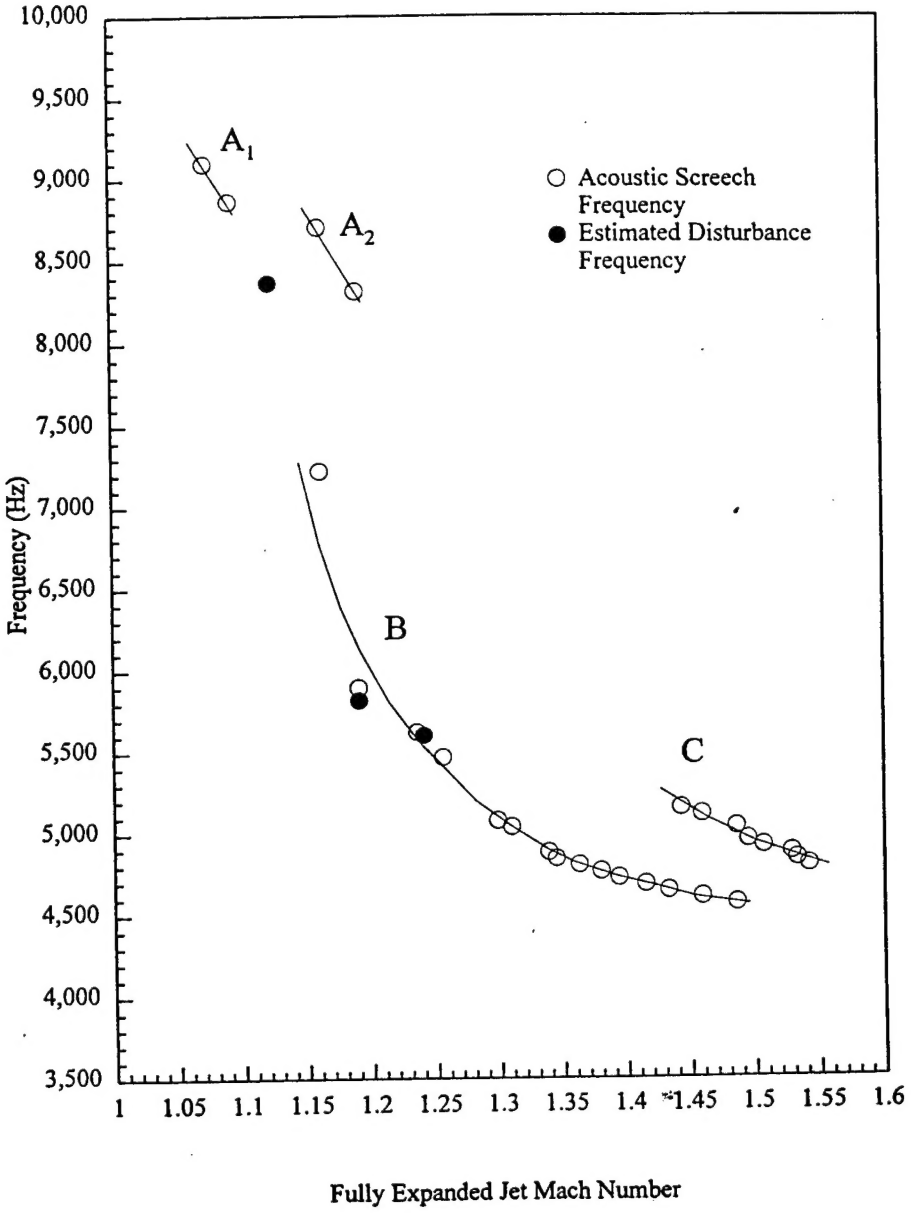

Figure 1. Screech Acoustic Frequency and its Comparison to Disturbance Frequency

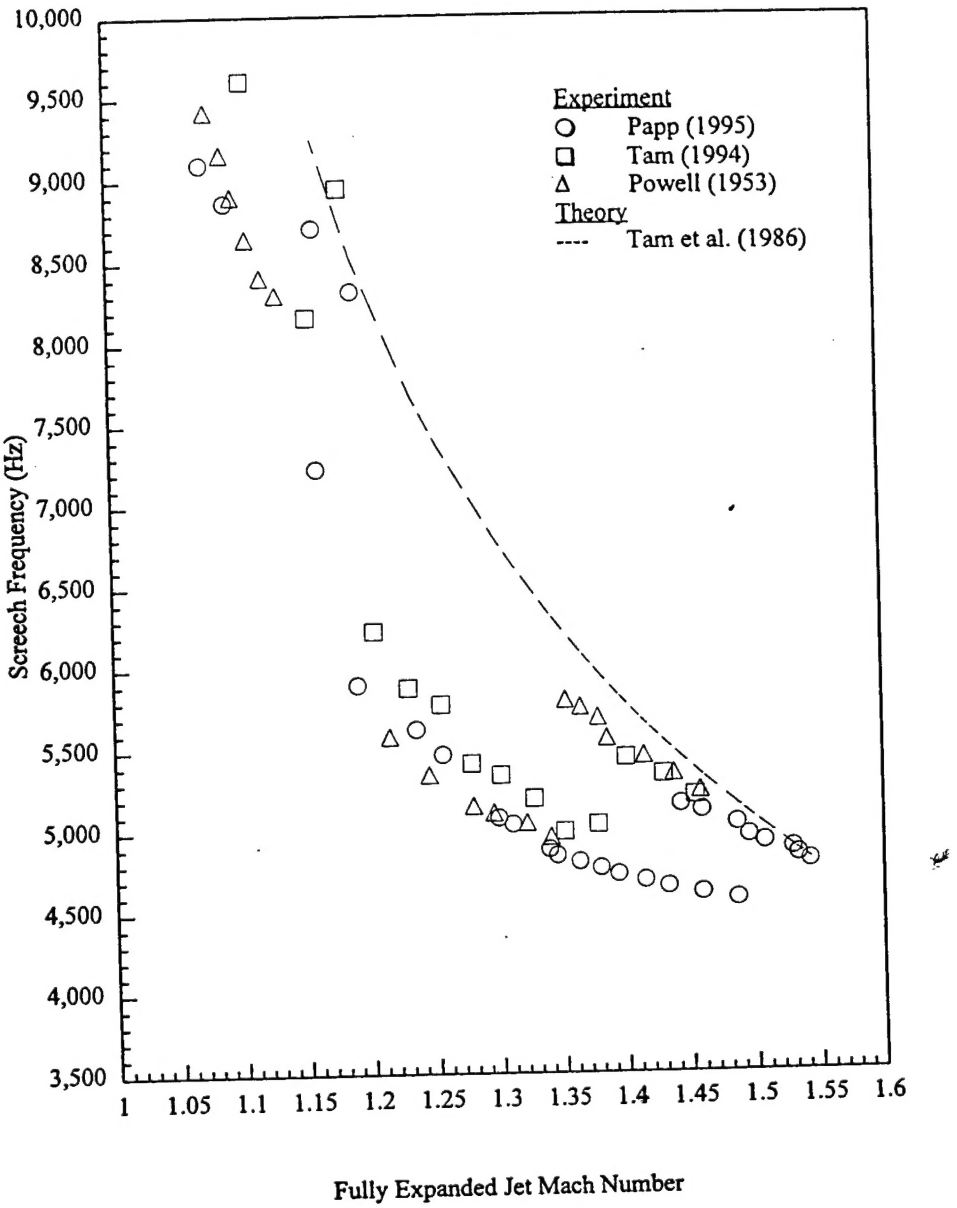

Figure 2. Comparison between Current and Published Screech Frequency Data

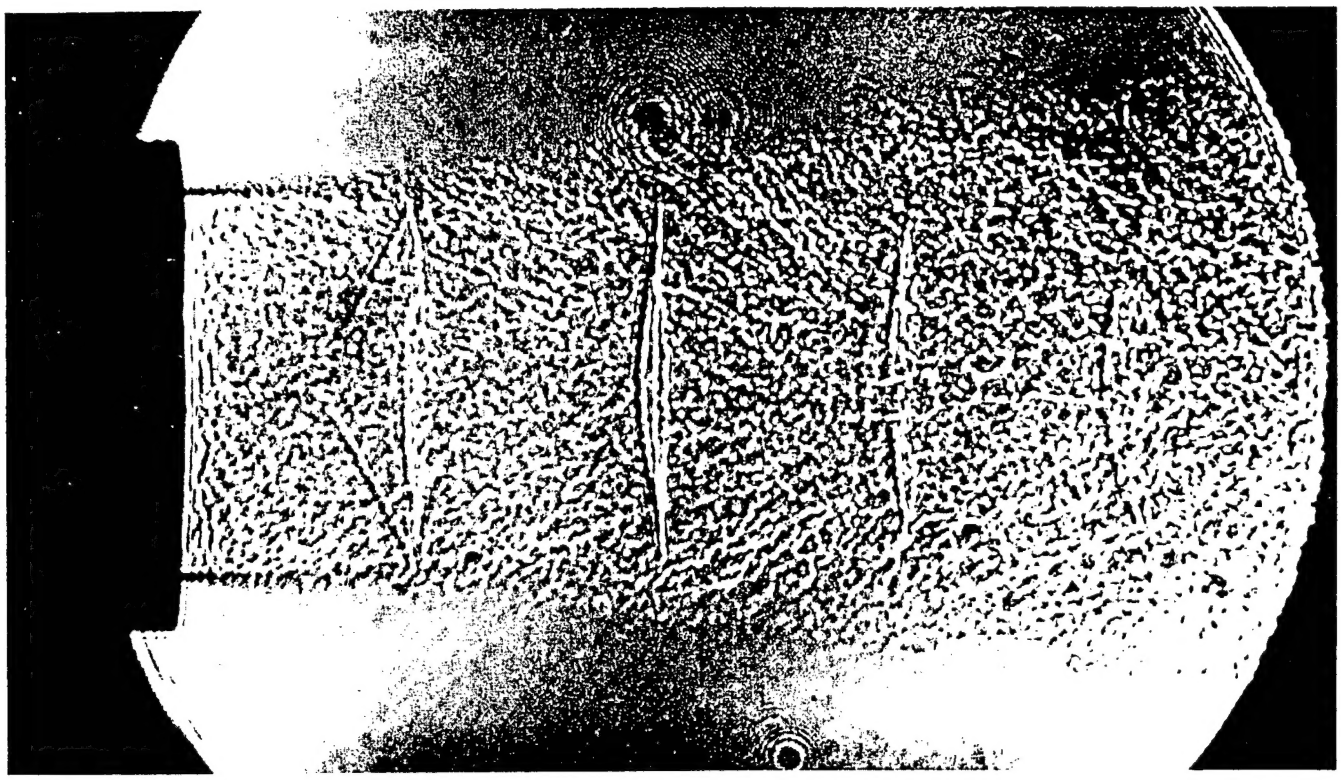

Figure 3. Nd-Yag Shadowgraph Image, $M_j = 1.12$

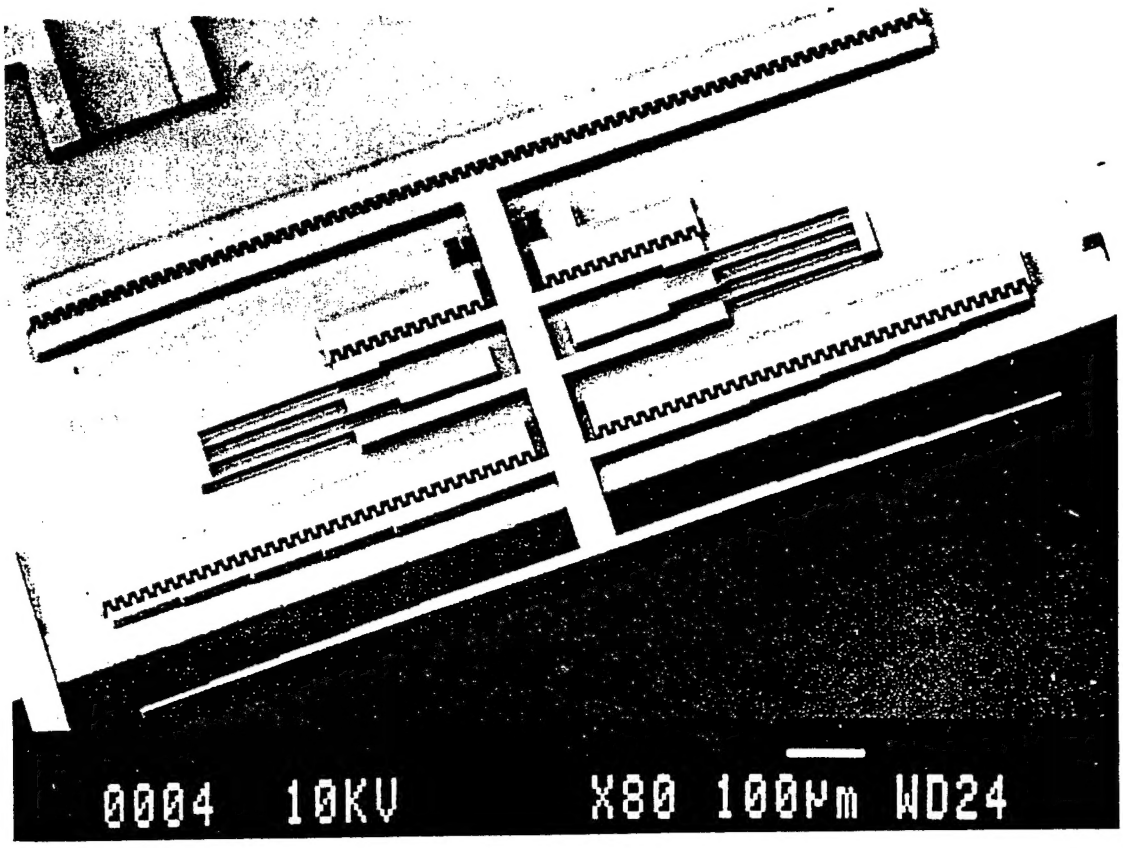

Figure 4. SEM Photograph of a First-Geneartion Actuator

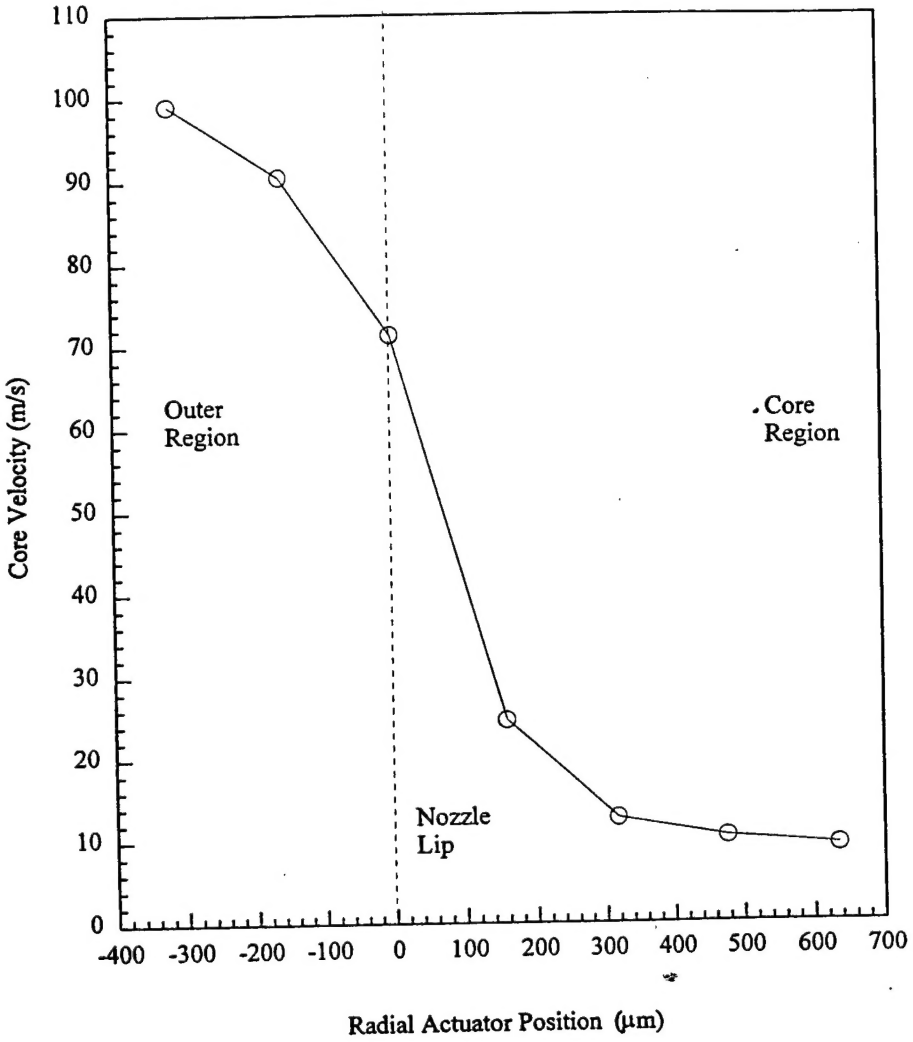

Figure 5. Jet Core Velocity Range of Maximum Amplitude Operation

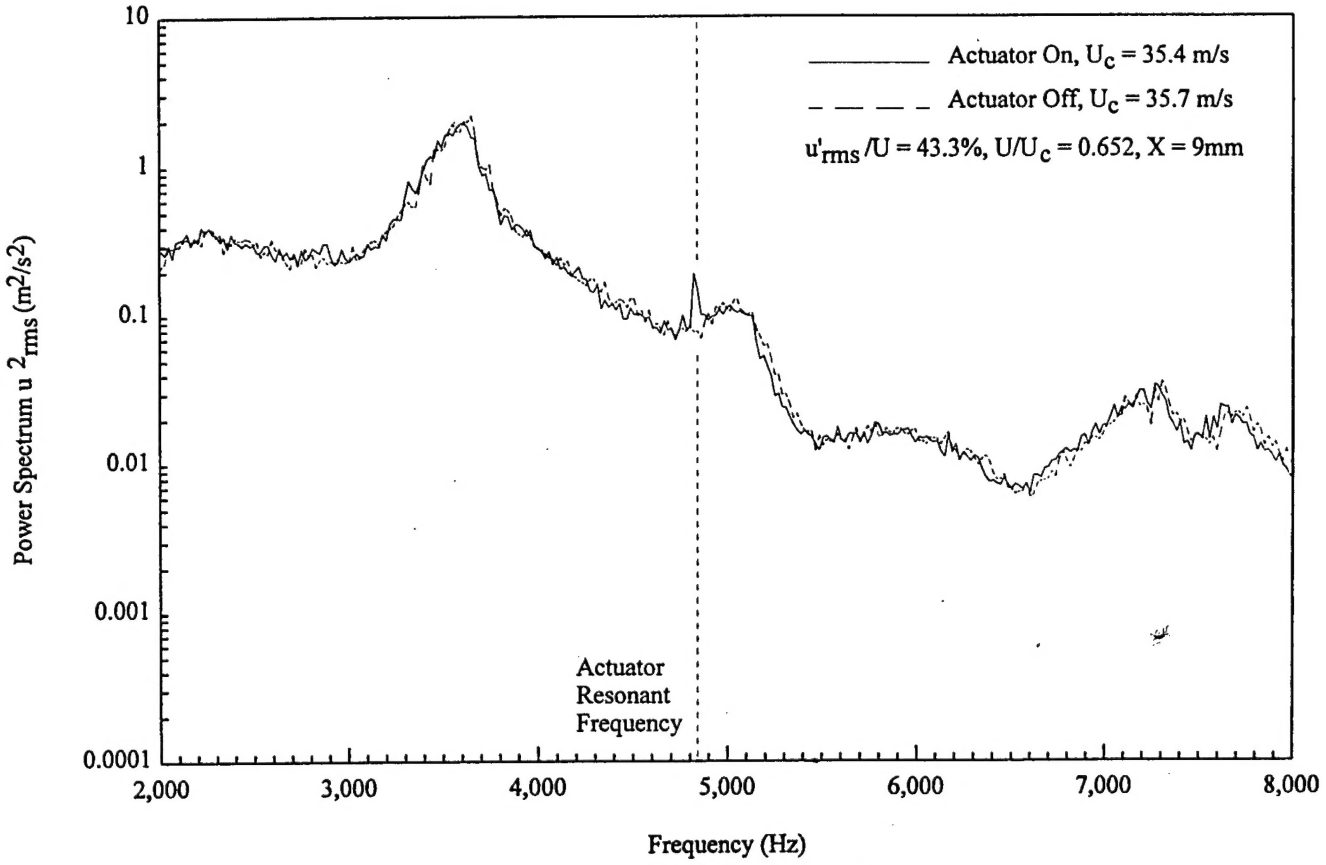

Figure 6. Shear Layer Velocity Spectra, U_J = 35.5 m/s

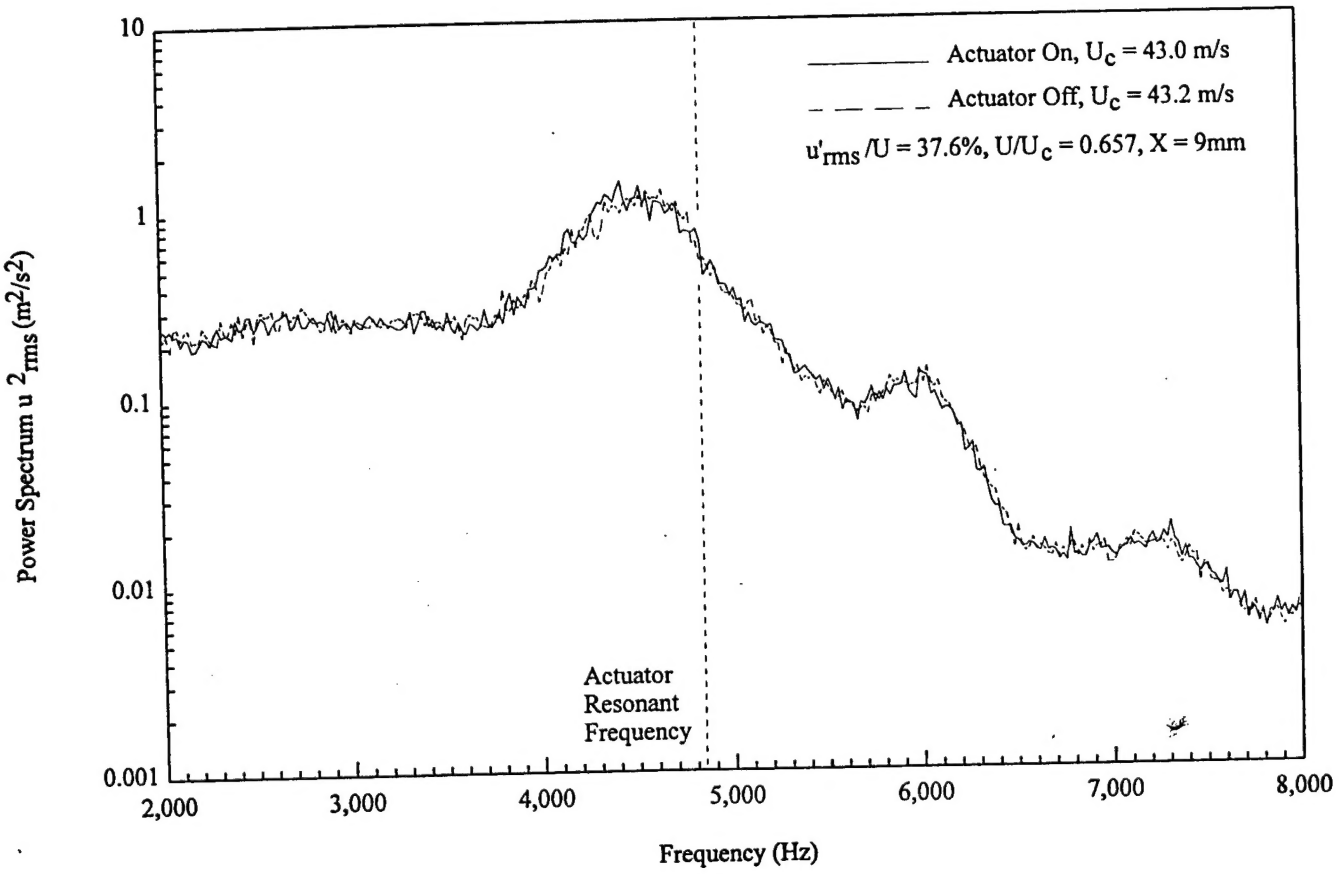

Figure 7. Shear Layer Velocity Spectra, U_j = 43 m/s

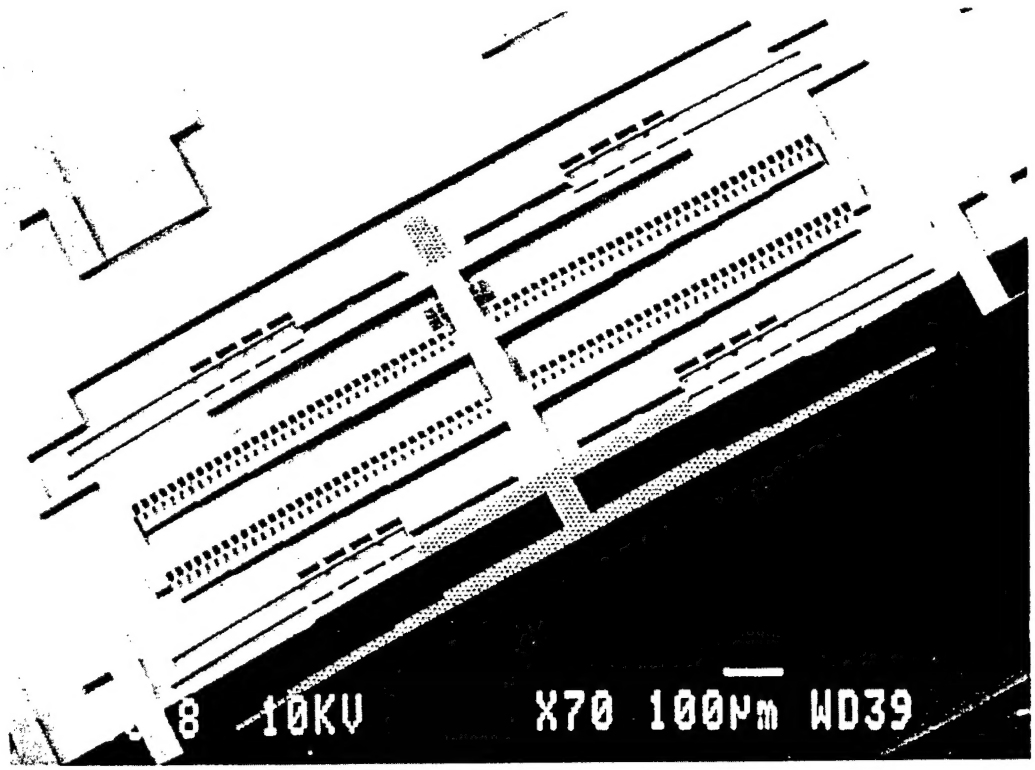

Figure 8. SEM Photograph of a Second-Generation MEMS Actuator